DJ Journal of Engineering Chemistry and Fuel, Vol. 2(1) 2017, pp. 10-20

RESEARCH ARTICLE

Synthesis and Characterization of Virgin and Ag doped CuO: SnO_2 Mixed Composites

R Jayaseelan[1], *M Gopalakrishnan[1]

[1]Department of Chemistry, Annamalai University, Annamalainagar – 608002, Tamilnadu, India.

Received- 2 October 2016, Revised- 20 December 2016, Accepted- 20 January 2017, Published- 28 January 2017

ABSTRACT

Nano metal oxides and binary composite of Ag doped and undoped CuO and SnO_2 nanoparticles have been synthesized by co-precipitation method and characterized by FT-IR, XRD, SEM, EDX and UV-Vis Spectral studies. XRD results show that the average crystalline size of metal oxides ranges from 13 to 32 nm. The presences of Sn-O bond in metal oxide have been observed from FT-IR measurements. Effect of silver nanoparticles on band gap changes for Nano crystalline SnO_2, CuO and CuO: SnO_2 composite has been also investigated. This has been done by finding the optical band gap from the absorption edge which is determined from UV measurement. XRD results suggest that the introduction of Ag in metal oxides and composites can increase the crystallinity of metal oxides and Nano composite and the average crystalline size of nanoparticles. EDX spectrum shows the purity of Ag doped CuO: SnO_2 nanocomposite. From the UV –Vis spectrum it has been clearly observed that silver doped and undoped CuO: SnO_2 nanocomposite shows the similar band gap value of Indium Tin Oxide (ITO).

Keywords: Nanoparticles, FT-IR, XRD, SEM, UV-Vis Spectroscopy.

1. INTRODUCTION

Gas sensing applications demand materials that offer a fast response speed, a fast recovery time and high sensitivity for trace level detection of various gases. [1] first reported the enhanced sensitivity of SnO_2 with CuO dopant for H_2S gas detection. The addition to SnO_2 (n-type semiconductor) of a second phase such as CuO (p-type semiconductor) gives rise to p-n junctions of which capacitance is sensitive to gaseous adsorption, leading to the possibility of a capacitive detection [2-5].

SnO_2 sensor loaded with CuO nanoparticles exhibits a fast response speed with a high sensitivity and quick recovery primarily due to the efficient dispersal of the CuO catalyst and its presence in the form of nanoparticles proffers a greater surface area on the SnO_2 film surface and simple SnO_2 film, mixed SnO_2-CuO composite layer, CuO/SnO_2 continuous bilayer, and evaporated CuO clusters on the SnO_2 structure [6-8].

Doping with CuO has been shown to enhance the sensitivity and selectivity of SnO_2 toward H_2S. In comparison to pure SnO_2, SnO_2: CuO films show a high resistivity in air which drastically drops in the presence of hydrogen sulfide or other sulfur compounds. This behaviour has been attributed to the formation of p–n heterojunctions (p-CuO and n-SnO_2), which induces an electron depleted space charge layer at the surface of SnO_2. Subsequent exposure to dry air brings the sulfide back to CuO and the p–n junctions are reconstructed [9].

The CuO/ SnO_2 element has been also tested for their sensitivity to other gases such as CO, CH_3SH, $(CH_3)_2S$, C_2H_5OH, H_2 etc. It shows very clearly that even for such a high concentration of these gases, the CuO/ SnO_2 element shows very small or negligible sensitivity compared to H_2S at an operating temperature of 100 ^oC, except for CH_3SH [10].

The novel nanosized CuO-SnO_2 photocatalyst have been prepared with the simple co-precipitation method. The CuO-SnO_2 photocatalyst calcined at 500 °C for 3 h (the molar ratio of Cu to Sn is 1:1) has been found to reach the highest photocatalytic

*Corresponding author. Tel.: +919442389644
Email address: profmgk61@gmail.com (M.Gopalakrishnan)
Double blind peer review under responsibility of DJ Publications
https://dx.doi.org/10.18831/djchem.org/2017011002

activity due to the sample with good crystallization and high BET surface area. The effective photo degradation dye by CuO-SnO_2 photocatalyst under simulated sunlight is a very exciting respect in photocatalytic area and this work may provide new insights into the development of novel sunlight photocatalysts [11].

2. EXPERIMENTAL

2.1. Preparation of pure and Ag doped CuO: SnO_2 Mixed Composites

The Nano sized CuO-SnO_2 mixed composite have been prepared by co-precipitation method. $SnCl_2.2H_2O$ and $CuSO_4.5H_2O$ have been used as the starting materials, and ammonia (1:1) has been used as the precipitator. A certain amount of $SnCl_2.2H_2O$ and $Cu(SO)_4.5H_2O$ at a mass ratio of w(CuO):w(SnO_2) = 90: 10 has been dissolved in de-ionized water to get a mixed aqueous solution. Before mixing of $SnCl_2.2H_2O$ precursor to $Cu(SO)_4.5H_2O$ solution, 1ml of con. HCl has been added with $SnCl_2.2H_2O$. Then $NH_3.H_2O$ has been added into the solution drop wise under the sonication process until transforming precipitation completely and keeps the pH value of the solution in the range of 10. Figure B1 shows the formation of Nano sized composite. The precipitate has been filtered and washed with deionized water until no SO_4^{2-} and Cl^- have been found in the filtrates. Aging has been done at 80 ^oC for 24 hrs. Then the wet powder has been dried at about 120 °C in air at 24 hrs to form the precursor of the CuO:SnO_2 composite. Finally the precursors have been calcinated for 3 h at 500 ^oC in air to prepare the Nano sized mixed composite. Then, we simply mixed untreated sol of CuO:SnO_2 composite with $AgNO_3$ salt solution under sonication to make Ag doped CuO:SnO_2 Nano composite. Finally, the wet powder has been dried at about 120 °C in air at 24 hrs to form the precursor and then dried powder have been calcinated for 3 h at 500 ^oC in air to prepare the Ag doped CuO:SnO_2 Nano composite powder. Figure B2 shows the formation of pure CuO:SnO_2 and Ag doped CuO:SnO_2 precipitates.

2.2. Measurements

IR spectra have been recorded in AVATAR-330 FT-IR spectrophotometer (Thermo Nicolet) and only noteworthy absorption levels (reciprocal centimeters) are listed. XRD patterns have been recorded for the centrifuged and dried samples using X–ray Rigaku diffractometer with Cu K_α source (30 kV, 100 mA), at a scan speed of 3.0000 deg/min, step width of 0.1000 deg, in a 2θ range of 20-80°. The Energy Dispersive X-ray (EDS) spectra of the Nano semiconductors have been recorded with a JEOL JSM-5610 Scanning Electron Microscope (SEM) equipped with Back Electron (BE) detector and EDX. The sample has been placed on an adhesive carbon slice supported on copper stubs and coated with 10 nm thick gold using JEOL JFC- 1600 auto fine coater prior to measurement. The nanoparticles has been recorded by using UV–Vis spectroscopy by employing a Systronics double beam UV–vis spectrophotometer operated on 200–800 nm wavelengths.

3. RESULTS AND DISCUSSION

3.1. FT-IR spectral studies

Several bands due to fundamentals, overtones and combinations of OH, Sn–O and Sn–O–Sn entities appear in the 4000–750 cm^{-1} range; below 750 cm^{-1} there occurs the cut off arising from lattice vibration. The IR spectrum of CuO: SnO_2 sample is seen to consist of peaks corresponding to those of pure SnO_2 and a single merged peak for CuO. In order to explore with a suitable resolution in the region 450–1500 cm^{-1}, the spectrum of a sample calcinated at 500 ^oC in air has been recorded after mixing in a KBr powder. The results and the proposed attributes are presented in table A1, Figure B3 shows the FT-IR spectrum in a range of 450–4000 cm^{-1}.

3.2. X-Ray Diffraction (XRD) studies

Figure B4 shows the X-ray powder Diffraction (XRD) pattern of the as-prepared SnO_2 calcinated at 500 ^oC. Compared to JCPDS (file No. 77-0452) standard pattern, the peaks are indexed as (110), (101), (200), (211), (220), (002), (310), (112), (301), (202) and (321) in the order of increasing diffraction angles, indicating a body centered tetragonal rutile crystalline structure of SnO_2 crystal. The peaks are apparently broad, showing that the small-sized Nano crystalline SnO_2 is obtained. The average crystal size of the resulting SnO_2 is around 13 nm, obtained using Scherrer's

equation based on the XRD peak broadening analysis. In addition, the peaks position of the (111) plane of CuO and (110) plane of SnO_2 have been also shifted to higher 2θ values due to doping of Ag content. Conclusively we can conclude that the big Ag ions have been added into the CuO and SnO_2 crystal planes [12].

Figure B4 shows the X-ray Diffraction (XRD) patterns of powder samples of Ag doped and undoped CuO: SnO_2 mixture containing 90 wt% of CuO and 10 wt% of SnO_2 and CuO, SnO_2 nanoparticles. The spectra for CuO and SnO_2 correspond to monoclinic and cassiterite structures (Joint Committee on Powder Diffraction Standards (JCPDS) card nos. 89-5899 and 77-0452 respectively) without any indication of other crystalline byproducts. The X-ray diffraction spectra for the CuO: SnO_2 samples annealed at 500 ^oC with 90% CuO loading shows monoclinic CuO along with the SnO_2 peaks, suggesting that CuO and SnO_2 are coexistent in the composites as separate phases. By raising the calcination temperature, the XRD spectrum shows sharper and more intensified CuO peaks, indicating an increase in the CuO grain size. However, increase in the calcination temperature beyond an optimum temperature leads to a decrease in the degree of crystallinity of the CuO phase. Crystallite size of Nano composite and nanoparticles have been measured by using DP calculator and from measured values, the average crystallite size is ranging from 13 - 32 nm. Table A2 shows the crystalline structures and the average crystalline sizes of Nano composite and nanoparticles.

The results of doping of silver on Nano composite and nanoparticles are summarised as follows,

i) The $\Delta\theta \approx 0.6^o$ Right shift in their XRD spectra which is mainly due to higher ionic radius (89 pm) of silver (Ag>Cu>Sn) atom.
ii) Doping of d-Block element (Ag) increase the crystallinity of SnO_2, CuO & $0.9CuO:0.1SnO_2$
iii) Doping of D-Block element increases the avg. crystalline size of nanoparticles

The X-ray diffraction spectra shows monoclinic phase of CuO along with CuS and Cu_2O peaks. Due to residual sulfur content, cubic (JCPDS card no. 89-2073) and hexagonal (JCPDS card no. 79-2321) phases of CuS exist along with the monoclinic phase of CuO. During calcination Cu^{2+} ion react with OH^- ion and it makes the Cu_2O cubic phase (JCPDS card no. 78-2076).

3.3. Scanning Electron Microscopy (SEM) and Energy Dispersive X-Ray Analysis (EDX)

The SEM image of figure B5 shows that the particles have been obtained in an agglomerated state. SEM analyses indicated that there have been large differences in microstructure between various samples. Some samples had much smaller grains with irregular sizes, but others had obvious bulk particles with irregular sizes. Figure B5 shows the micrograph of Nano composites and nanoparticles. It is observed that the powder prepared by the ultrasonic assisted co-precipitation method has a flake structure. The composition of a single particle is difficult to be quantitatively determined because of its small particle size. Figure B5 (a & b) represents pure SnO_2 and CuO respectively and figure B5 (c) represents Ag doped $0.9CuO:0.1SnO_2$ Nano composite. The results of energy dispersive X-ray analysis (Figure B6) of the composite powders show that the sample contains four kinds of elements, Ag, Cu, Sn and O. In the sample, the content 6.6% (mass fraction) of residual sulfur (S) is present. It is mainly due to the improper reduction of CuO from $CuSO_4$ precursor. In powder form particles are in an agglomerated state due to the specific gravity of the particles but in the liquid phase, particles are uniformly dispersed which is shown from the DLS particle size analysis. From particle size analysis we can conclude that the nanoparticles and Nano composites have average diameters ranging from 39 to 92 nm.

3.4. UV-VIS spectral studies

UV–Visible absorbance spectra of the Nano composite and Nano materials investigated can be seen in figure B7. As is evident from figure B7, the silver colloid showed a clear and distinct Surface Plasmon (SP) resonance band at 427 nm. But doping of silver on CuO shows the shifting of cut off wavelength from 278.7 to 285 nm which exhibited an immediate red-shift of about 6.3 nm. In the same way doping of silver on SnO_2 shows the shifting of the cut off wavelength from 339.5 to 355.3 nm which exhibited an

immediate red-shift at about 15.8 nm. In silver doped CuO: SnO_2, Nano composite shows the shifting of cut off wavelength from 284.3 to 287.4 nm which exhibited an immediate red-shift at about 3.1 nm. But there is no SP resonance band shift observed from UV-Vis spectrum of Nano composite. Based on these reflectance spectra the absorption edge for each compound has been determined. Using these absorption edge values, the band gap energy has been calculated from equation in each instance (Table A3) [13, 14]. $E_g = h^*C/ \lambda_c$ where, h = Planks constant = 6.626 x 10^{-34} J s, C = Speed of light = 2.998 x 10^8 m/s, λ_c = Cut off wavelength in nm, [1eV = 1.602 X 10^{-19} J (conversion factor)].

4. CONCLUSIONS

Nano metal oxides and binary composite have been prepared by using co-precipitation method and characterized by XRD, FT-IR, SEM, EDX and UV-Vis Spectroscopy. It can be seen from XRD results that the average crystalline size of metal oxides and composite powder are ranging from 13 to 32 nm. The presence of Cu-O and Sn-O bonds in metal oxides and composites has been observed from FT-IR measurements. Effect of silver nanoparticles on band gap changes for Nano crystalline SnO_2, CuO and CuO: SnO_2 composite have also been investigated. This has been done by finding the optical band gap from the absorption edge determined from UV measurement. XRD results suggest that the introduction of Ag in metal oxides and composites can increase the crystallinity of metal oxides and Nano composite and average crystalline size of nanoparticles. EDX spectrum shows the purity of the Ag doped CuO: SnO_2 Nano composite. From the UV –Vis spectrum it has been clearly observed that silver doped and undoped CuO: SnO_2 Nano composite shows the similar band gap value of Indium Tin oxide (ITO). Due to this similarity in band gap, it is possible to replace the existing material ITO with the prepared Nano composite. Band gap tuning of Nano composite has been achieved through doping of silver ion. Higher band gap value of the silver doped and undoped Nano composite may improve the efficiency of the photovoltaic as well as gas sensor applications.

5. ACKNOWLEDGMENTS

We are thankful to Mr. D. Jayaseelan, PSG, Coimbatore for providing the instrumentation facility.

REFERENCES

[1] Tomoki Maekawa, Jun Tamaki, Norio Miura and Noboru Yamazoe, Sensing Behavior of CuO-Loaded SnO_2 Element for H_2S Detection, Chemistry Letters, Vol. 20, No. 4, 1991, pp. 575-578, http://doi.org/10.1246/cl.1991.575.

[2] J.Roman, J.C.Fabian, M.Labeau and G.Delabouglise, Synthesis, Structure, and Gas Sensitivity Properties of SnO_2–CuO Mixture Phase Obtained by Pyrolysis of an Aerosol, Journal of Materials Research, Vol. 12, No. 2, 1997, pp. 560-565, https://doi.org/10.1557/JMR.1997.0080.

[3] Abdul Majid, James Tunney, Steve Argue, David Kingston, Michael Post, James Margeson and Graeme J.Gardner, Characterization of CuO phase in SnO_2–CuO prepared by the modified Pechini method, Journal of Sol-Gel Science and Technology, Vol. 53, No. 2, 2010, pp. 390-398, http://dx.doi.org/ 10.1007/s10971-009-2108-x.

[4] M.Jayalakshmi and K.Balasubramanian, Hydrothermal Synthesis of CuO-SnO_2 and CuO-SnO_2-Fe_2O_3 Mixed Oxides and their Electrochemical Characterization in Neutral Electrolyte, International Journal of Electrochemical Science, Vol. 4, No. 4, 2009, pp. 571-581.

[5] Jinhuai Liu, Xingjiu Huang, Gang Ye, Wei Liu, Zheng Jiao, Wnaglian Chao, Zhongbai Zhou and Zenglian Yu, H_2S Detection Sensing Characteristic of CuO/SnO_2 Sensor, Sensors, Vol. 3, No. 5, 2003, pp. 110-118, http://dx.doi.org/10.3390/s30500110.

[6] Lifang He, Yong Jia, Fanli Meng, Minqiang Li and Jinhuai Liu, Development of Sensors Based on CuO-doped SnO_2 Hollow Spheres for ppb Level H_2S Gas Sensing, Journal of Materials Science, Vol. 44, No. 16, 2009, pp. 4326-4333, http://dx.doi.org/10.1007/s10853-009-3645-y.

[7] MA Ming-you, HE Ze-qiang, XIAO Zhuo-bing, HUANG Ke-long, XIONG Li-zhi and WU Xian-ming, Synthesis and Electrochemical Properties of SnO_2-CuO Nanocomposite Powders, Transactions of Nonferrous Metals Society of China, Vol. 16, No. 4, 2006, pp. 791-794, http://dx.doi.org/doi:10.1016/S1003-6326(06)60327-0.

[8] Arijit Chowdhuri, Vinay Gupta, K.Sreenivas Rajeev Kumar and Subho Mozumdar P.K.Patanjali, Response Speed of SnO_2-Based H_2S Gas Sensors with CuO Nanoparticles, Applied Physics Letters, Vol. 84, No. 7, 2004, pp. 1180-1182, http://dx.doi.org/10.1063/1.1646760.

[9] Abdul Majid, Tunney, Steve Argue, David Kingston, Michael Post, James Margeson and Graeme J.Gardner, Characterization of CuO phase in SnO2–CuO prepared by the modified Pechini method, Journal of Sol-Gel Science and Technology, Vol. 53, No. 2, 2010, pp. 390-398, http://dx.doi.org/10.1007/s10971-009-2108-x.

[10] Jinhuai Liu, Xingjiu Huang, Gang Ye, Wei Liu, Zheng Jiao, Wnaglian Chao, Zhongbai Zhou and Zenglian Yu, H_2S Detection Sensing Characteristic of CuO/SnO_2 Sensor, Sensors, Vol. 3, No. 5, 2003, pp. 110-118, http://dx.doi.org/ 10.3390/s30500110.

[11] XIA Hui-li , ZHUANG Hui-sheng , ZHANG Tao and XIAO Dong-chang, Photocatalytic Degradation of Acid Blue 62 over CuO-SnO_2 Nanocomposite Photocatalyst under Simulated Sunlight, Journal of Environmental Sciences, Vol. 19, No. 9, 2007, pp. 1141-1145.

[12] S.H.Jeong, B.N.Park, S.B.Lee and J.H.Boo, Structural and Optical Properties of Silver-Doped Zinc Oxide Sputtered Films, Surface and Coatings Technology, Vol. 193, No. 1, 2005, pp. 340-344, http://dx.doi.org/10.1016/j.surfcoat.2004.08.112.

[13] P.G.L.Baker, R.D.Sanderson and Andrew Crouch, Sol–Gel Preparation and Characterisation of Mixed Metal Tin Oxide Thin Films, Thin Solid films, Vol. 515, No. 17, 2007, pp. 6691-6697, http://dx.doi.org/10.1016/j.tsf.2007.01.042.

[14] K.I.Dhanalekshmi and K.S.Meena, Ag@Tio2 Core-Shell Nanoparticles as Antifungal Agents: Synthesis, Characterization and Antifungal Activity Screening, DJ Journal of Engineering Chemistry and Fuel, Vol. 1, No. 4, 2016, pp. 52-59, http://dx.doi.org/10.18831/djchem.org/2016041005

APPENDIX A

Table A1.IR band positions and fundamental vibrations

ν (cm^{-1})	**Fundamental vibrations**
780 - 450	stretching vibration of Metal–Oxides (CuO & SnO_2)
1000 - 450	vibration band of Cu-O
1200 - 450	vibration band of PVA capped Silver
1631,1633	vibration band of $–NO_3$ impurities
3423,3430	stretching vibration of the surface hydroxyls (-OH) stretching vibration of the adsorbed water

Table A2.XRD results of nanocomposite and nanoparticles

Sample	**Crystal structure**	**Lattice**	**Average crystalline size(nm)**	**JCPDS Ref No.**
SnO_2	Tetragonal	Primitive	13	77-0452
CuO	Monoclinic	End -centered	20	89-5899
Ag/CuO	Monoclinic	End -centered	21	89-5899
CuO:SnO_2	Tetragonal / Monoclinic	Primitive / End -centered	29	89-5899 77-0452
Ag/ CuO:SnO_2	Tetragonal & Monoclinic	Primitive & End -centered	22	77-0452 89-5899

Table A3.Absorption edges and band gap energies of nanocomposites and nanoparticles

Compound	**Absorption Edge (nm)**	**Band Gap Energy (Eg) in eV**		
		Measured	**Bulk Size**	**Nano Size**
SnO_2	339.5	3.65	3.6	4.2
CuO	278.7	4.45	1.2-1.5	2.55
CuO:SnO_2	284.3	4.36	-	3.03
Ag/CuO:SnO_2	287.4	4.31	-	-

APPENDIX B

Figure B1.Colloidal silver nanoparticles formation

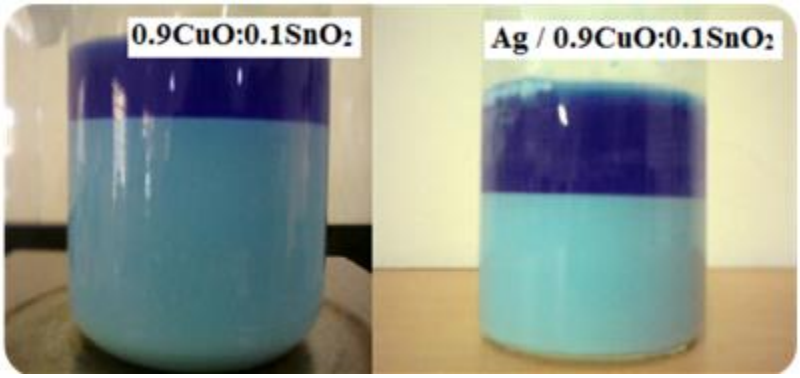

Figure B2.Ag doped and undoped CuO: SnO_2 precipitate formation

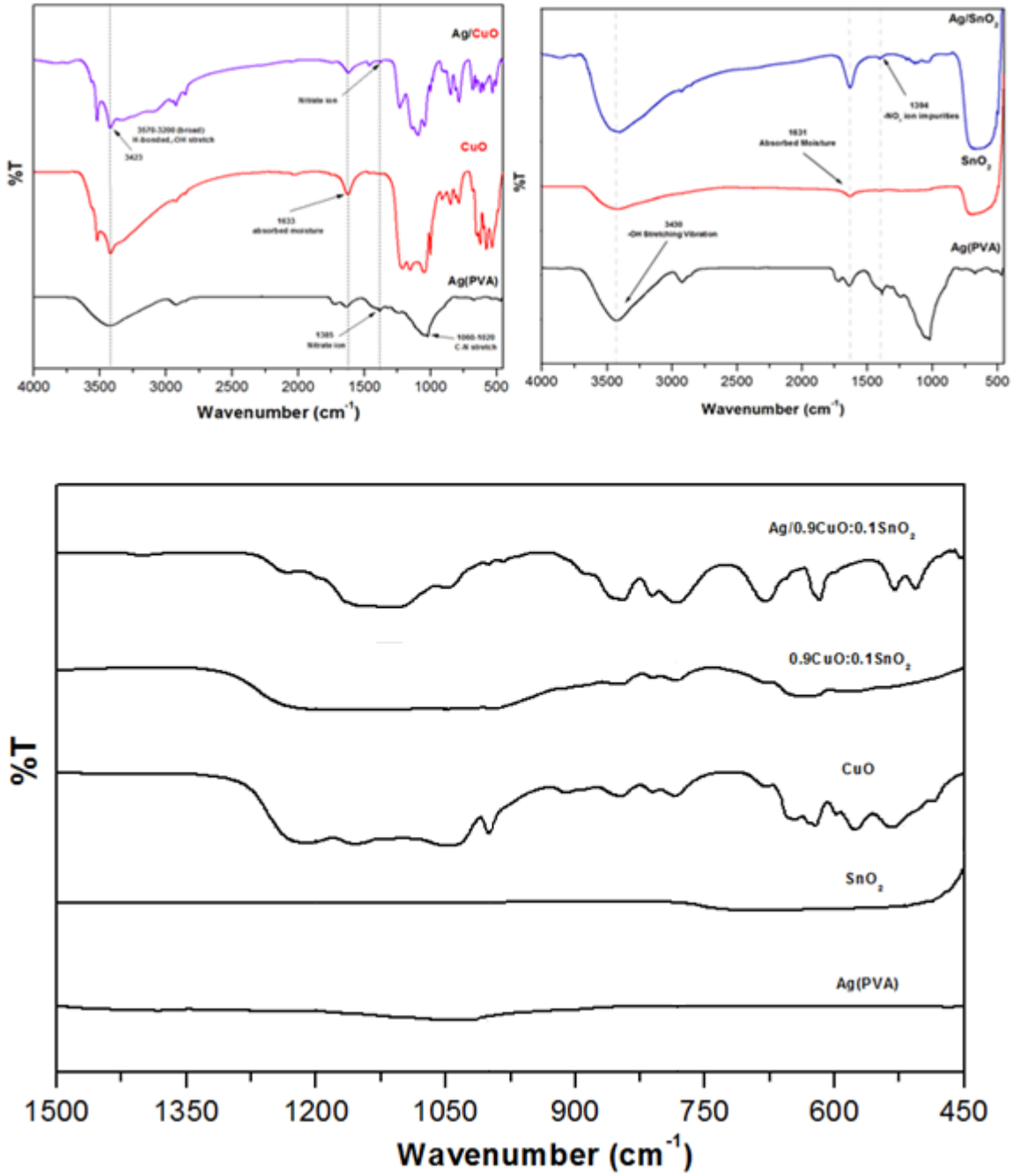

Figure B3.FT-IR spectra of Ag doped and undoped CuO: SnO_2 nanocomposites and CuO, SnO_2 nanoparticles

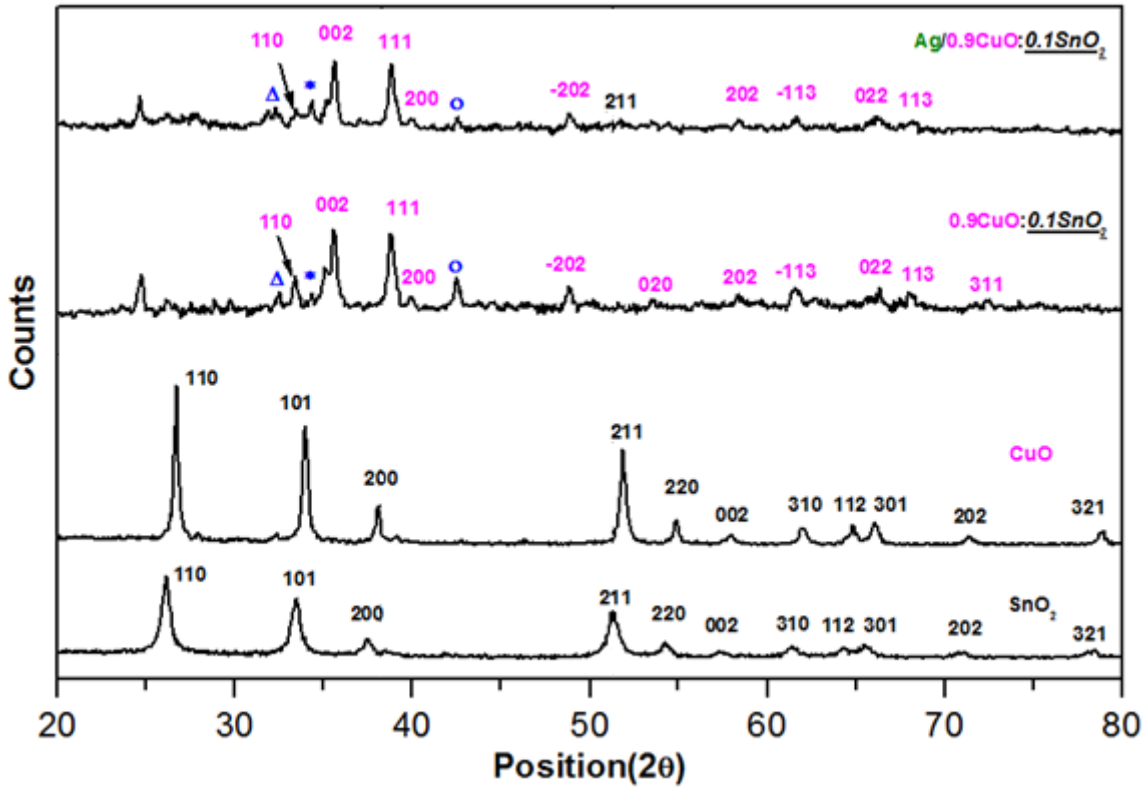

Figure B4.XRD pattern of Ag doped and undoped CuO: SnO_2 nanocomposites and CuO, SnO_2 nanoparticles

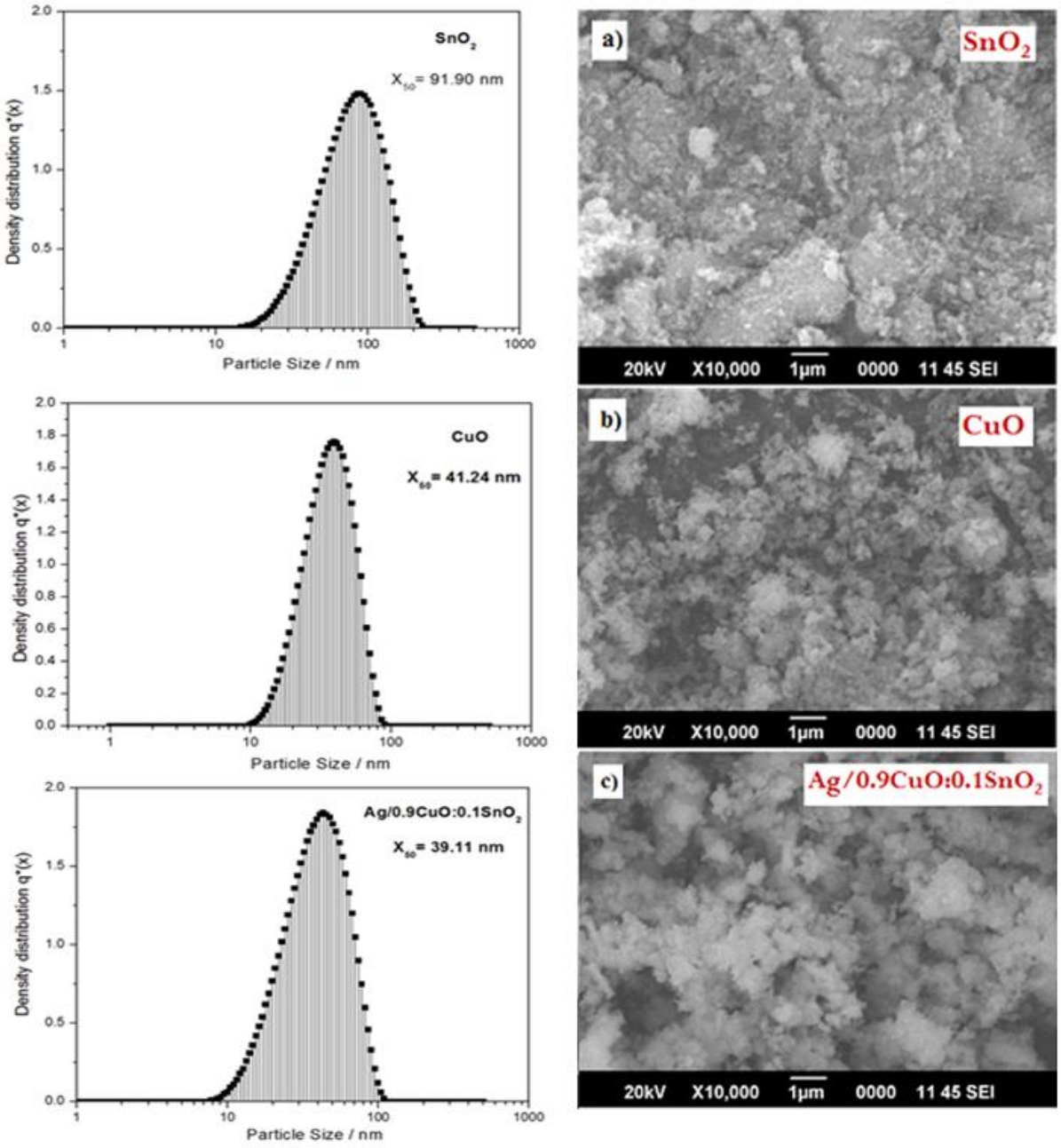

Figure B5.SEM images of (a & b) pure SnO_2 and CuO respectively, (c) Ag doped CuO:SnO_2 nanocomposite

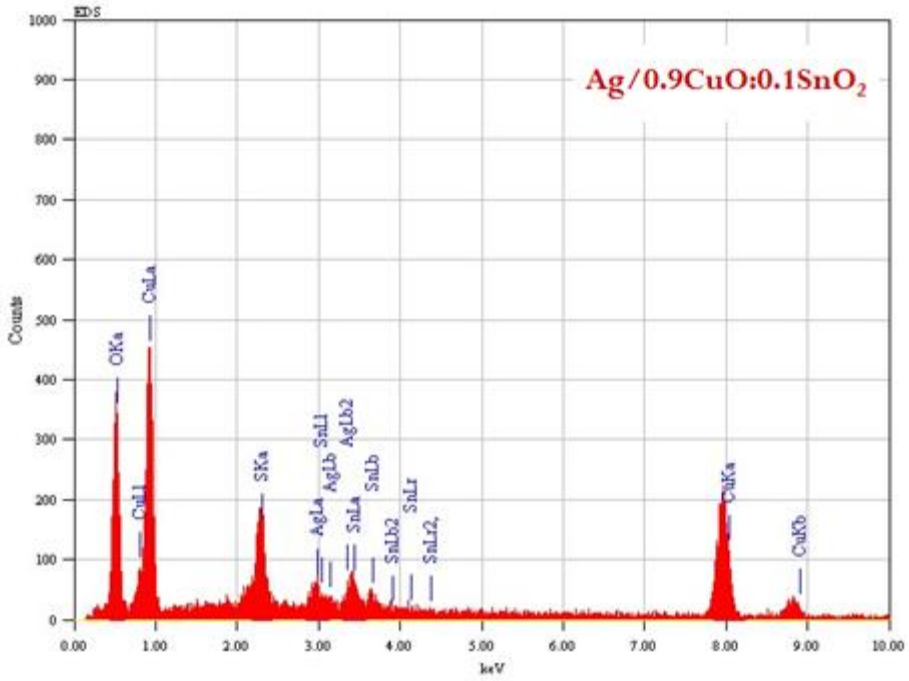

Figure B6.EDX spectra of Ag doped CuO: SnO_2 nanocomposite

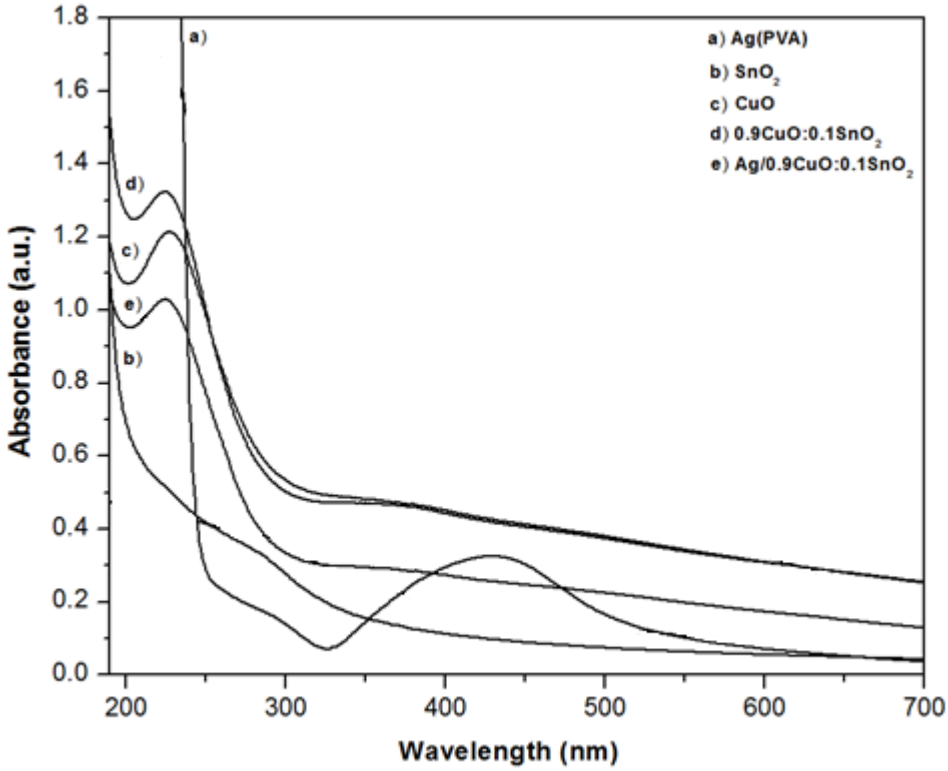

Figure B7.UV–Visible spectra of the nanocomposites and nanoparticles